Supporting Information

Face-Rich Au Nanoparticles Govern the Size Dependence of Photocatalytic Methane Coupling on TiO_2

Chunwei Yuan[a,1], Zhijun Zhang[a,1], Xin Liu[a], Songrun Qin[a], Lun He[a], Tianqi Yu[a], Xiang Yu[b], Bang Gu*[a], Wenhao Fang*[a, c]

[a] *School of Chemical Science and Technology, Yunnan University, 2 North Cuihu Road, Kunming 650091, China.*

[b] *State Key Laboratory of Alternate Electrical Power System with Renewable Energy Sources, School of Electrical and Electronic Engineering, North China Electric Power University, Beijing 102206, China.*

[c] *School of Chemistry and Chemical Engineering, Henan Normal University, Xinxiang 453007, China.*

[1] *C. Yuan and Z. Zhang contributed equally to this work*

[*] *Correspondence authors.* Bang Gu, E-mail: gubang@ynu.edu.cn; Wenhao Fang, E-mail: wenhao.fang@ynu.edu.cn.

Experimental Methods

Preparation of TiO_2. Anatase was calcined in a tubular furnace (heating rate 2°C min^{-1}, H_2 30 mL min^{-1}, 600 °C for three hours) to obtain the TiO_2 support.

Loading gold nanoparticles as a co-catalyst. Au nanoparticles (NPs) were loaded onto TiO_2 as a co-catalyst by the H_2 reduction method. In brief, 100 mg of TiO_2 was suspended in 30 ml of $HAuCl_4$ aqueous solution (0.2 mL 5 mg mL^{-1} $HAuCl_4 + H_2O$). The suspension was stirred in an 80°C water bath and evaporated to dryness. Subsequently, the resulting powder was calcined in a tubular furnace under a H_2 atmosphere (heating rate 2°C min^{-1}, at X °C for 1 hour, X = 200, 300, 400, 500, 600), and then ground to obtain Au/TiO_2 with different Au nanoparticle sizes.

Characterization methods. X-ray diffraction (XRD) analysis was performed on a Bruker D8 Advance diffractometer with Cu Kα radiation and a beam voltage of 40 kV. The patterns were registered in the 2θ domain of 10-90 ° at a screening rate of 10 ° min^{-1}. Transmission electron microscopy (TEM) was carried out on a field-emission JEOL-2100 F system with an acceleration voltage of 200 kV. The dispersion of Au could be estimated using the empirical relationship between particle distribution (D) and average particle size (d).

$$D = \frac{6 \times n_s \times M}{\rho \times N_A \times d}$$

where n_s is the number of atoms at the surface per unit area (1.15×10^{19} m^{-2} for Au), M is the molecular weight (196.97 g mol^{-1} for Au), ρ is the density (19.5 g cm^{-3} for Au), N_A is 6.023×10^{23} mol^{-1}, and d is the average particle size measured by TEM.

Energy dispersive spectroscopy (EDS) elemental mapping was conducted on an X-MaxN 80 T IE250 at 200 KV. Photoluminescence spectroscopy (PL) was recorded on an Edinburgh Instruments FSL980 with 200-1700 nm steady-state spectrum. The excited wavelength was fixed at 480 nm. X-ray photoelectron spectroscopy (XPS) was carried out on a Thermo Scientific Kα+ system equipped with Al Kα radiation under ultrahigh vacuum. The binding energy shift due to the surface charging was adjusted with a reference of the C 1 s line at 284.8 eV. Ultravioletvisible diffuse reflectance spectrum (UV-vis DRS) was recorded on a Shimadzu UV3600 apparatus.

Photoelectrochemical (PEC) performance of the catalyst was analyzed on an AutoLab electrochemical workstation model no. PGSTAT302N using a standard three-electrode cell. Indium tin oxide (ITO) glass deposited by the catalyst was used as the working electrode, a saturated calomel electrode (SCE) was used as the reference electrode, and a Pt wire was used as the counter electrode. To prepare the working electrode, 5 mg of catalyst was dispersed into 0.5 mL of ethanol, and then 10 μL of Nafion® solution was added and the mixture was sonicated for 2 h to make it homogeneous. Afterwards 10 μL of the mixed droplets were coated on the ITO glass with a controlled area of 0.25 cm^2, followed by drying at room temperature for 30 min to form a film electrode. The photoelectrochemical test was conducted under a 300 W xenon lamp, and a Na_2SO_4 solution (0.5 mol L^{-1}, 100 mL, pH = 6.8, 25 ^oC) was used as the electrolyte.

Photocatalytic test. A 95 mL custom-made quartz reactor was used to evaluate the performance of photocatalytic CH_4 conversion. Typically, 2.5 mg of as-prepared photocatalyst was dispersed in 1 mL of ethyl alcohol via sonication and uniformly dropped onto a pre-cleaned quartz substrate (1.5 × 1.5 cm). After drying at 313 K, the quartz substrate was horizontally placed in the reactor. Subsequently, the reactor was purged with CH_4 (99.999%) for 10 min. A 300 W xenon lamp (CEL-HXUV300-T3, Beijing China Education Au-light Co., Ltd.) was used to irradiate the reactor from top with light intensity of 1000 mW cm^{-2}. The reacted gas was analyzed by a gas chromatograph (GC2060, N_2 carrier) equipped with thermal conductivity detector (TCD) and flame ionization detector (FID) to quantify H_2, CO, CO_2 products and hydrocarbons.

The performance parameters were calculated according to the following equations:

$$CH_4\ conversion\ rate = [2 \times n(C_2H_6) + 2 \times n(C_2H_4) + 3 \times n(C_3H_6) + 3 \times n(C_3H_8) + n(CO) + n(CO_2)]/m/t$$

$$CH_4\ conversion = [2 \times n(C_2H_6) + 2 \times n(C_2H_4) + 3 \times n(C_3H_6) + 3 \times n(C_3H_8) + n(CO) + n(CO_2)]/n(CH_4) \times 100\%$$

$$C_2\ selectivity = [2 \times n(C_2H_6) + 2 \times n(C_2H_4) + 3 \times n(C_3H_6) + 3 \times n(C_3H_8)]/[2 \times n(C_2H_6) + 2 \times n(C_2H_4) + 3 \times n(C_3H_6)$$

$$+ 3 \times n(C_3H_8) + n(CO) + n(CO_2)] \times 100\%$$

The initial intrinsic turnover frequency (TOF) of surface Au atoms on each catalyst was then calculated according to the following formula.

$$TOF = \frac{v \times M}{a \times D}$$

where v is the reaction rate, M is the molecular weight (196.97 g mol^{-1} for Au), a is Au mass percentage, and D is the dispersion of Au.

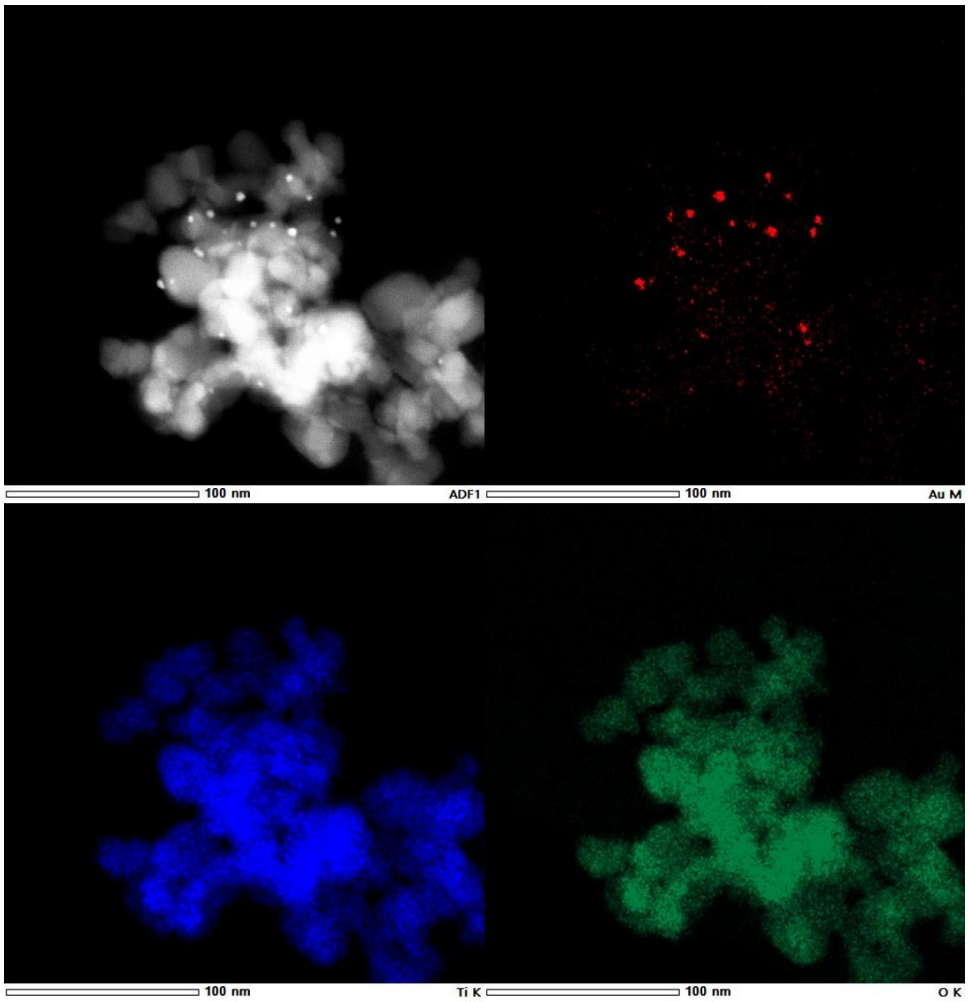

Fig. S1. HAADF STEM image and EDS elemental mapping of Au (red), Ti (blue), and O (green) elements of Au/TiO_2 (7.8 nm).

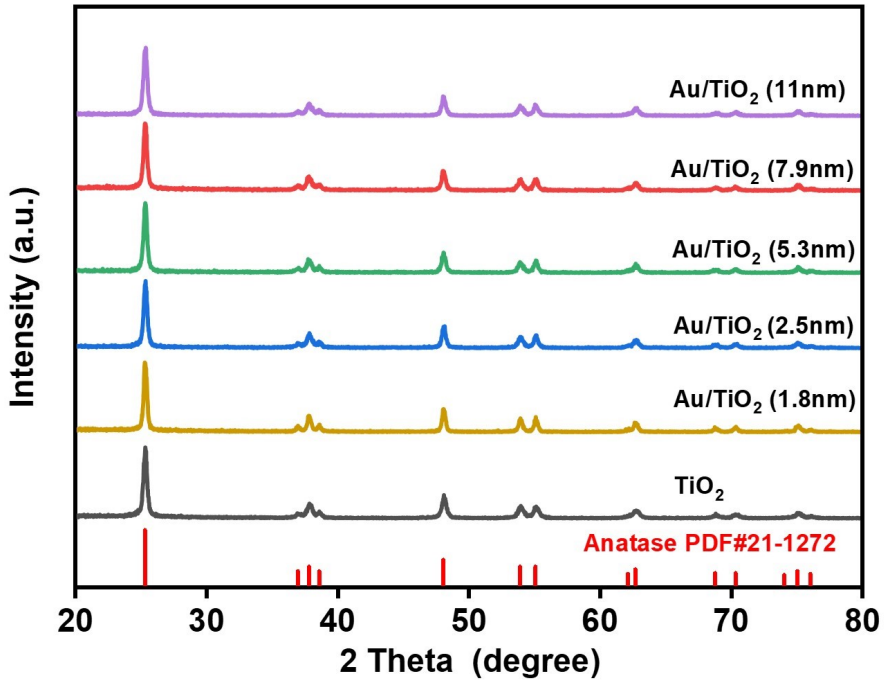

Fig. S2. XRD patterns of Au/TiO_2 catalysts.

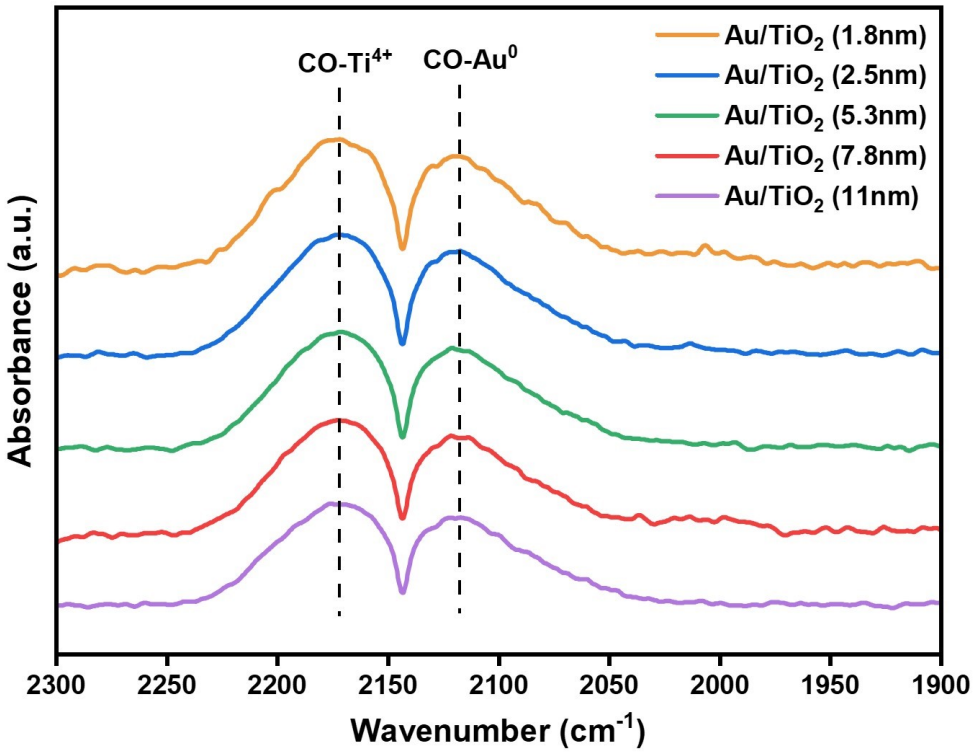

Fig. S3. CO Fourier transform infrared spectra of Au/TiO_2 catalysts.

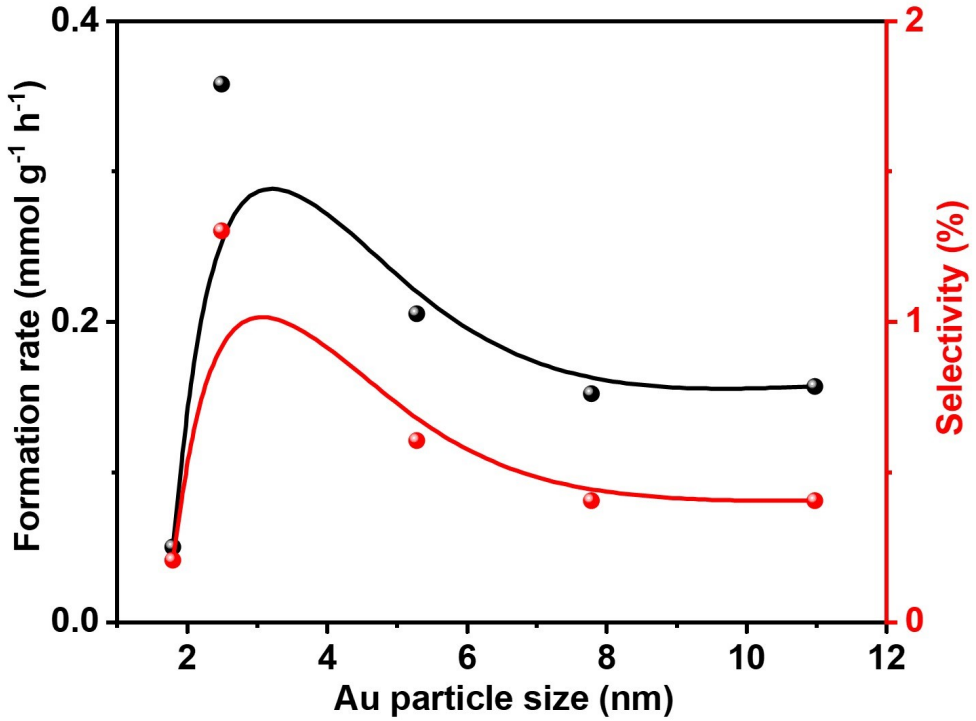

Fig. S4. CO selectivity and production of Au/TiO_2 catalysts.

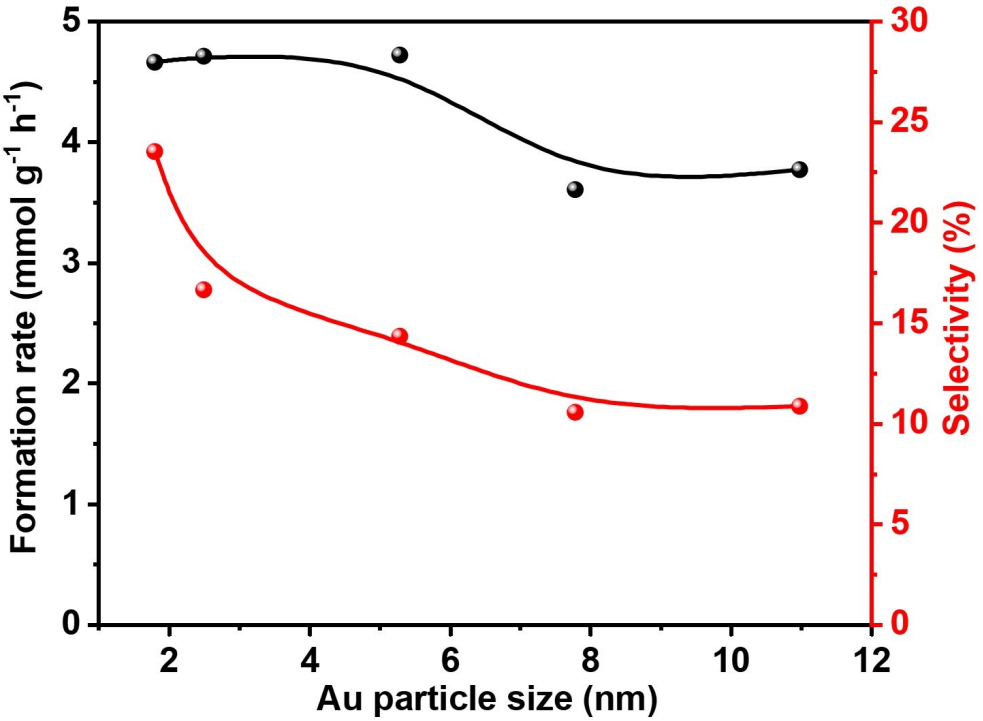

Fig. S5. CO_2 selectivity and production of Au/TiO_2 catalysts.

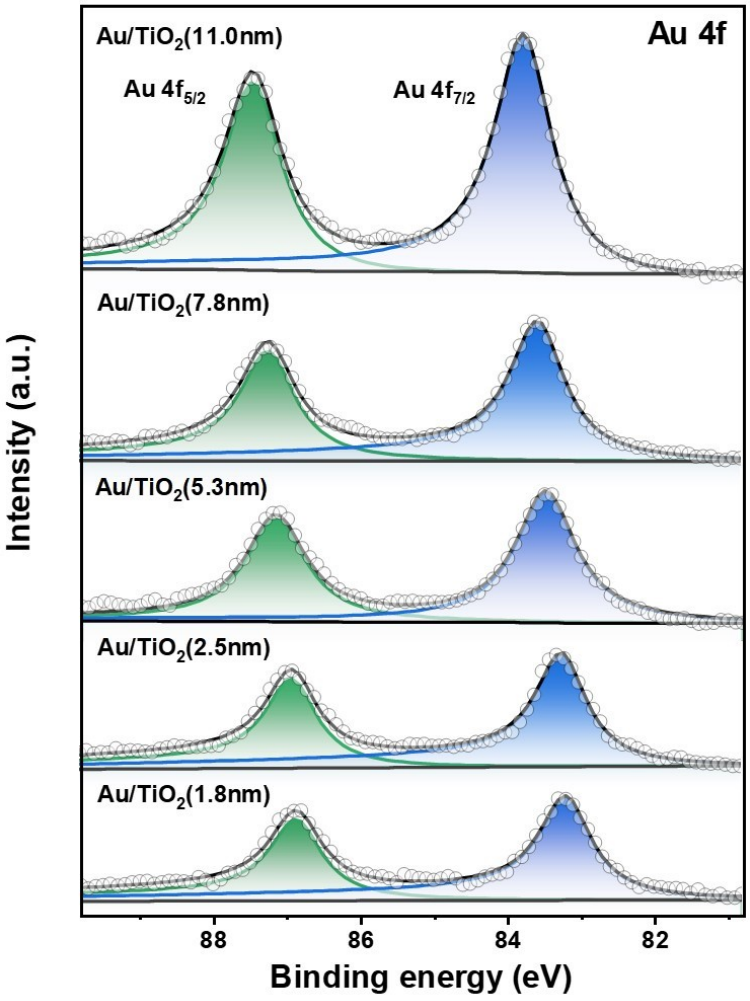

Fig. S6. Au 4f XPS patterns of Au/TiO_2 catalysts.

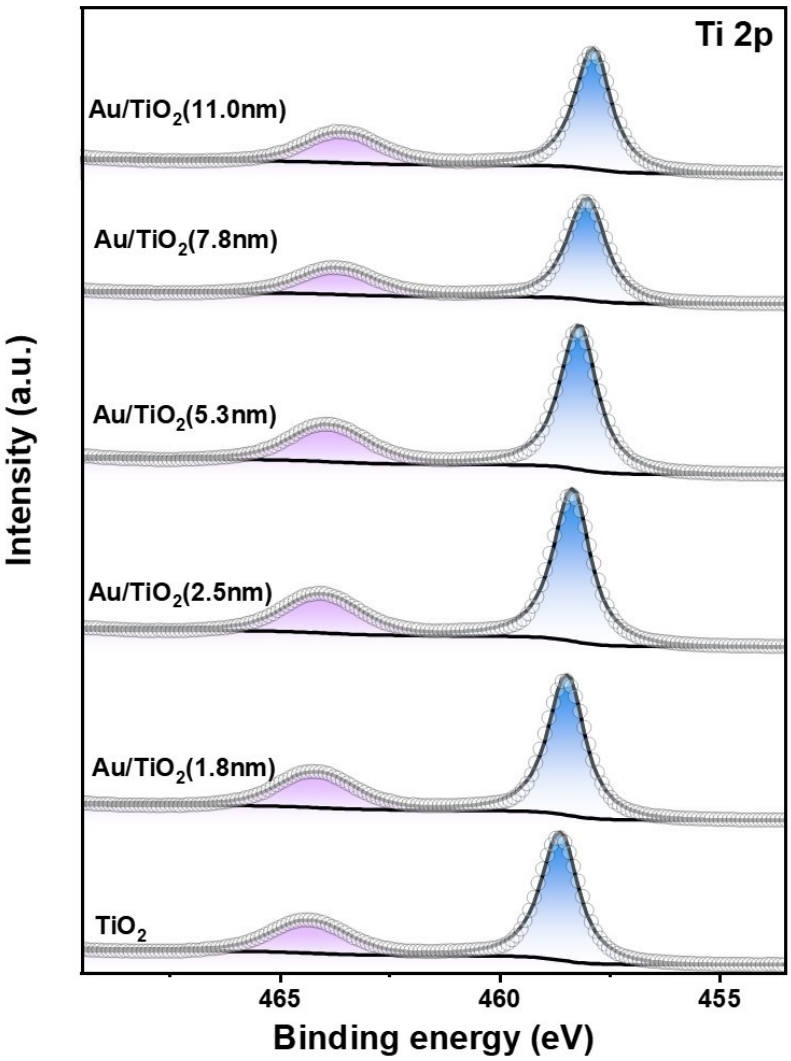

Fig. S7. Ti 2p XPS patterns of Au/TiO_2 catalysts.

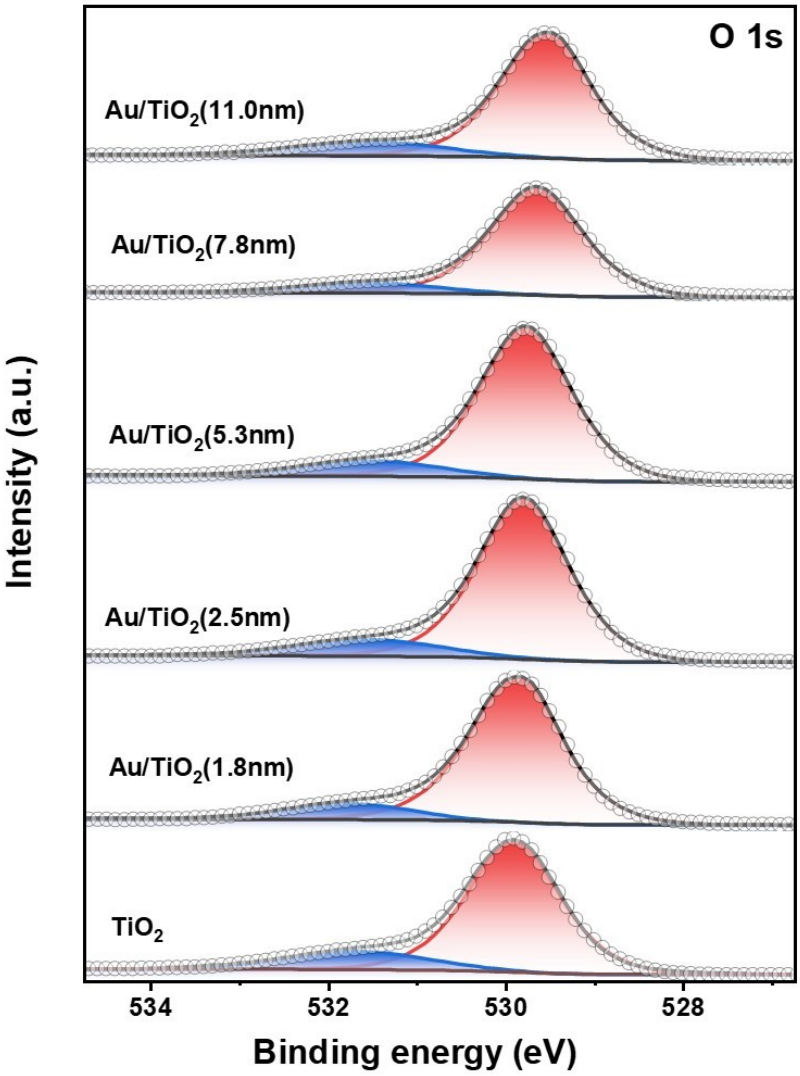

Fig. S8. O 1s XPS patterns of Au/TiO_2 catalysts.

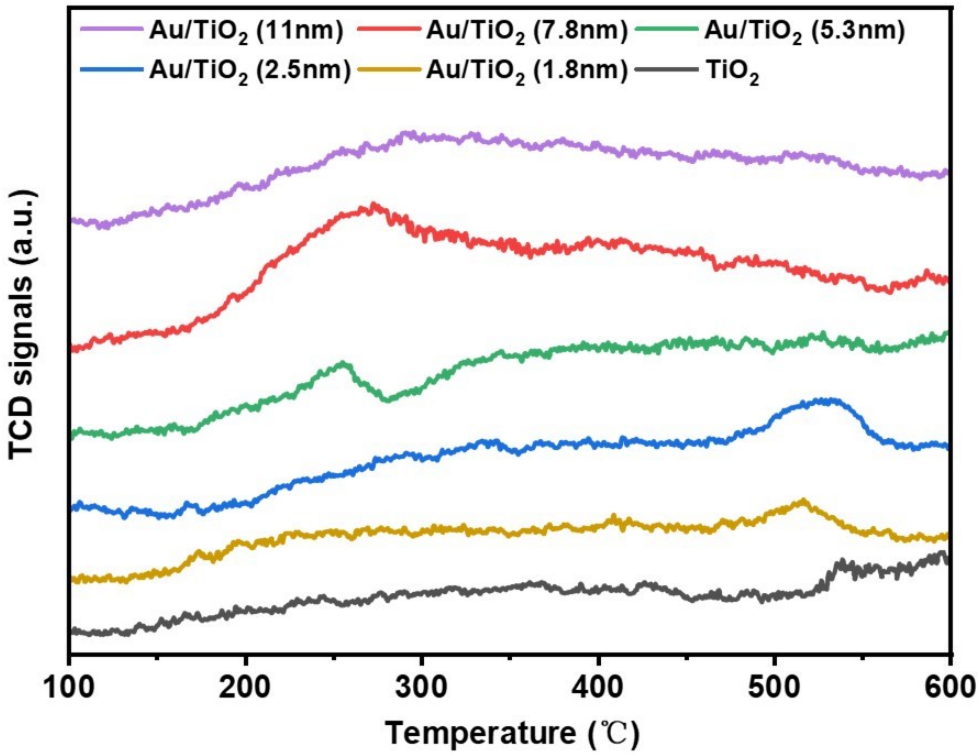

Fig. S9. O_2-TPD patterns of Au/TiO_2 catalysts.

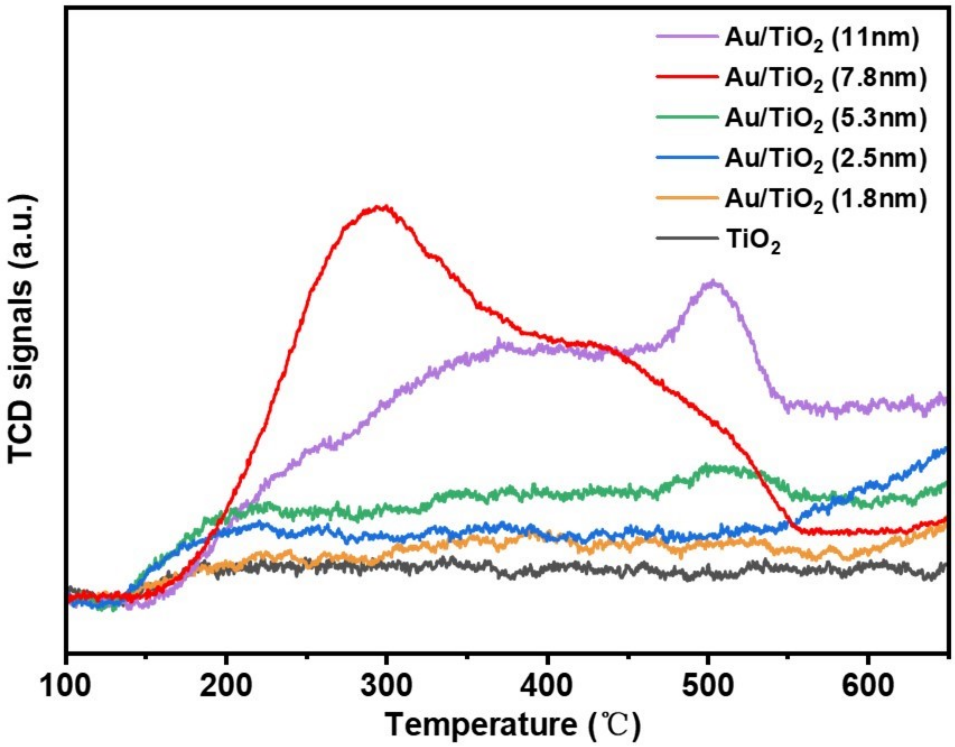

Fig. S10. CH_4-TPD patterns of Au/TiO_2 catalysts.

Table S1. *in situ* DRIFT-IR spectra of CO adsorption of CO-Au^0 peak area of Au/TiO_2 catalysts.

Au particle size(nm)	CO-Au^0 peak area
1.8	5.79
2.5	5.38
5.3	5.31
7.8	5.19
11	4.52

Table S2. Photocatalytic OCM performance over Au/TiO_2 with different Au particle size.

Au particle size (nm)	Select. (%)							Prod. (mmol g^{-1} h^{-1})						
	C_2H_4	C_2H_6	C_3H_6	C_3H_8	C_2+	CO	CO_2	C_2H_4	C_2H_6	C_3H_6	C_3H_8	C_2+	CO	CO_2
1.8	1.9	69.5	0.4	4.5	76.3	0.2	23.5	0.19	6.89	0.03	0.30	7.41	0.05	4.66
2.5	2.2	72.4	0.8	6.8	82.1	1.3	16.6	0.31	10.25	0.07	0.64	11.27	0.36	4.71
5.3	2.2	75.3	0.8	6.8	85.1	0.6	14.3	0.37	12.45	0.08	0.75	13.65	0.20	4.72
7.8	2.3	79.1	0.9	6.8	89.1	0.4	10.5	0.39	13.61	0.11	0.77	14.88	0.15	3.60
11	2.2	78.1	1.1	7.4	88.8	0.4	10.8	0.39	13.66	0.12	0.87	15.04	0.16	3.77

Table S3. The results of blank experiments for photocatalytic OCM reaction over Au/TiO_2 (7.8nm).

Entry	Reactant	Catalyst	Light	Products
1	Ar	√	√	None
2	CH_4	×	√	None
3	CH_4	√	×	None
4	CH_4	√	√	C_2H_6

Table S4. Dispersion, C_2+ producibility, TOF, and the fraction of face, edge, corner Au atoms of Au/TiO_2 catalysts.

Au particle size(nm)	Dispersion (%)	C_2+ prod. (mmol g^{-1} h^{-1})	TOF (h^{-1})	Face (%)	Edge (%)	Corner (%)
1.8	64.3	7.41	607.5	26.2	62.7	11.1
2.5	46.3	11.27	1205.9	45.2	49.5	5.3
5.3	21.8	13.65	2977.2	73.4	25.5	1.1
7.8	14.8	14.88	4559.2	81.9	17.6	0.5
11	10.5	15.04	6727.8	87.1	12.7	0.2

Table S5. Photocatalytic OCM performance over Au/TiO_2 (7.8 nm) with different flow rate. (CH_4: 5% O_2/N_2 = 39:1)

Flow rate	**Select. (%)**							**Prod. (mmol g^{-1} h^{-1})**						
(mL min^{-1})	C_2H_4	C_2H_6	C_3H_6	C_3H_8	C_2+	CO	CO_2	C_2H_4	C_2H_6	C_3H_6	C_3H_8	C_2+	CO	CO_2
20	2.3	79.1	0.9	6.8	89.1	0.4	10.5	0.39	13.61	0.11	0.77	14.88	0.15	3.60
30	2.2	88.2	0.5	2.5	93.4	0.4	6.2	0.43	17.22	0.06	0.33	18.04	0.13	2.43
40	3.3	89.1	0.3	2.0	94.7	0.2	5.1	0.75	20.16	0.04	0.31	21.26	0.10	2.30
50	3.6	88.6	0.1	2.6	94.9	0.1	5.0	0.75	18.59	0.02	0.36	19.72	0.06	2.09

Table S6. Photocatalytic OCM performance over Au/TiO_2 (7.8 nm) with different CH_4 and 5% O_2/N_2 flow ratio with a total flow rate of 40 mL min^{-1}.

Flow ratio	Select. (%)							Prod. (mmol g^{-1} h^{-1})						
	C_2H_4	C_2H_6	C_3H_6	C_3H_8	C_2+	CO	CO_2	C_2H_4	C_2H_6	C_3H_6	C_3H_8	C_2+	CO	CO_2
39:1	3.3	89.1	0.3	2.0	94.7	0.2	5.1	0.75	20.16	0.04	0.31	21.26	0.10	2.30
38:2	2.9	85.9	0.5	3.8	93.1	0.2	6.6	0.70	21.02	0.09	0.62	22.43	0.12	3.24
39:3	2.9	84.7	0.4	3.9	91.9	0.3	7.8	0.79	23.10	0.08	0.71	24.68	0.17	4.25
36:4	2.1	83.8	0.5	4.0	90.4	0.4	9.2	0.59	24.08	0.09	0.77	25.53	0.21	5.30

Table S7. Photocatalytic OCM performance over Au/TiO_2 (7.8 nm) under different irradiation wavelengths. (catalyst 2.5 mg; time 2 h; CH_4 19.5 mL min^{-1}; 5% O_2/N_2 0.5 mL min^{-1})

Light wavelength (nm)	**Select. (%)**							**Prod. (mmol g^{-1} h^{-1})**						
	C_2H_4	C_2H_6	C_3H_6	C_3H_8	C_2+	CO	CO_2	C_2H_4	C_2H_6	C_3H_6	C_3H_8	C_2+	CO	CO_2
200-780	2.3	79.1	0.9	6.8	89.1	0.4	10.5	0.39	13.61	0.11	0.77	14.88	0.15	3.60
200-420	2.5	81.1	0.4	3.6	87.6	0.4	12.0	0.31	10.11	0.03	0.30	10.75	0.10	3.00
420-780	7.8	70.2	1.5	11.7	91.2	1.0	7.8	0.08	0.72	0.01	0.08	0.89	0.02	0.16